International Journal of Engineering

Journal Homepage: www.ije.ir

Influence of Water Cooling on Orthogonal Cutting Process of Ti-6Al-4V Using Smooth-Particle Hydrodynamics Method

M. Dehghani, A. R. Shafiei*

Department of mechanical Engineering, Yazd University, Yazd, Iran

P A P E R I N F O

Paper history:
Received 15 January 2019
Received in revised form 06 June 2019
Accepted 05 July 2019

Keywords:
Orthogonal Cutting Process
Cooling
Smooth Particle Hydrodynamic

A B S T R A C T

Temperature control during the cutting process with different parameters such as cutting velocity and applying water cooling is essential to decrease the cutting force, increase the life of the cutting tool and decrease the machined surface temperature of work-piece. In this research, the temperature of machined surface and the chip-tool interface in orthogonal cutting process of Ti-6Al-4V were investigated using smooth particle hydrodynamics (SPH) method. The effects of cooling with different speeds and temperatures of water flow on the temperature of these surfaces were studied. The non-cooling model is validated using experimental results. According to the results, a water flow with speed of 0.25 m/s at 20°C temperature causes a significant decreasing in the cutting force and the temperature on machined surface and chip-tool interface.

***doi**: 10.5829/ije.2019.32.08b.18*

1. INTRODUCTION

Cutting material from the extra parts of the work-piece is a cutting process to make a desirable geometric shape. Rising the temperature of this process increases tool wear [1], wasting energy [2], decrease the tool life [3] and affects on the surface roughness [4]. Safari et al. [5] investigated effects of turning parameters (spindle speed, feed and depth of cut) on surface roughness variation in dry machining of 55Cr3 steel bars. In orthogonal cutting process the temperature of machined surface and chip-tool interface vary by different conditions such as cutting speed and variations of cooling process.

The analytical models of cutting process are based on experimental observations such as cutting force and chip shape variations [6–8]. Unknown parameters of this model are obtained using experimental tests. The numerical methods such as finite element (FE) and SPH method analyze cutting process using mechanical properties of cutting tool and work-piece. FE method is based on the deformation and stress distribution of the cutting tool and the work-piece elements. Therefore, large deformation and material separation are important problems. These problems don't occur while analyzing the cutting process using SPH method because this method is mesh less and the work-piece is analyzed using nodes. Madaj and Piska [9] compared simulation results of the orthogonal cutting process of A2024-T351 aluminum alloy using SPH method with the experimental and FE ones. Limido et al. [10] used the ANSYS LS- DYNA solver to simulate this process with the Johnson-Cook and rigid material constitutive model to simulate work-piece and cutting tool respectively. Li et al. [11] proposed set of milling parameters to analyze the machining of titanium alloy by coated cemented carbide cutting tool using FE method. Heinstein and Segalman [12] simulated orthogonal cutting process using SPH method. They used the elastic and plastic hardening power constitutive material model of Stone et al. [13] to model the cutting tool and work-piece respectively. Also the cutting and trust forces were obtained using the SPH method [14]. Lu et al. [15] proposed a numerical two-dimensional coupled thermo-mechanical model of plane strain orthogonal cutting process. Cotterell et al. [16] measured temperature

*Corresponding Author Email: *arshafiei@yazd.ac.ir* (A. R. Shafiei)

Please cite this article as: M. Dehghani, A. R. Shafiei, Influence of water cooling on orthogonal cutting process of Ti-6Al-4V using Smooth-Particle Hydrodynamics method, International Journal of Engineering (IJE), IJE TRANSACTIONS B: Applications Vol. 32, No. 8, (August 2019) 1210-1217

during chip formation in orthogonal cutting process of Ti-6Al-4V using simple theoretical model according to Ernest-Merchand theory and two-dimensional thermal conductivity. They used the thermal and high speed camera to verify this thermal model. The probability of burning was investigated during the milling process of magnesium alloy [17] using thermal imaging. Also the thermocouple is used to investigate temperature distribution in cutting process [18, 19]. Making setup of this method is harder than thermal imaging method and its accuracy is lower. The temperature of machined surface of magnesium is maintained under melting temperature [20] using cooling process. Surface roughness of magnesium alloy [21] decreases with air flow rate at room temperature during the machining process. Heigel et al. [22] measured the temperature of the tool-chip interface while machining Ti-6Al-4V using infrared measurement.

Most mentioned studies ignored temperature distribution at work-piece while analyzing cutting process. The others validate the temperature distribution of numerical methods using experimental chip morphology and the cutting force. In this paper, temperature of machined surface and chip-tool interface are investigated using SPH method. The temperature on chip-tool interface is validated using experimental temperature. Then the cooling orthogonal cutting process with water flow is studied using the SPH method to find the influence of temperature and speed of water flow on the machined surface temperature.

2. SPH FORMULATION FOR SOLID FLOWS

Basic principles of the SPH method were introduced by the Monaghan in astronomical physics issues [23]. This method was expanded to solve fluid mechanics [24] and solids problems [25]. So far, many authors used this method to solve mechanical problems such as dynamic elastic problems [26] and plastic deformations [27], high velocity impact [28] and cold rolling process [29].
The integral representation of the function $f(x)$ at x_i is:

$$f\left(x_i\right) \approx \int_{\Omega} f\left(x\right) W\left(x - x_i\right) dA \tag{1}$$

Where Ω is integration area on A and W is kernel function. The derivative of the Equation (1) is

$$\frac{\partial f}{\partial x}\left(x_i\right) \approx -\int_{\Omega} f\left(x\right) \frac{\partial W\left(x - x_i\right)}{\partial x} dA \tag{2}$$

The integral representation of Equation (2) at discrete area is a summation of

$$\frac{\partial f}{\partial x}\left(x_i\right) = -\sum_{j \in \Omega} f_j \frac{\partial W\left(x_j - x_i\right)}{\partial x_\beta} A_j \tag{3}$$

Therefore derivative of the function f at x_i of particle i is approximated by summing the f_j (the value of function f at particle j as the neighbor of particle i) where Aj is area of a particle j and equals to m_j/ρ_j, m_j and ρ_j are mass and density of particle j. By using these definitions, Equation (4) is derived from Equation (3).

$$\frac{\partial f}{\partial x}\left(x_i\right) = \sum_{j \in \Omega} f_j \frac{\partial W_{ij}}{\partial x_\beta} \frac{m_j}{\rho_j} \tag{4}$$

Where $W_{ij}=W(x_i-x_j)$.
Mass conservation Equation (5) is expressed in particle summation as Equation (6) using particle approximation of Equation (4).

$$\frac{d\rho}{dt} = -\rho \frac{\partial v_\beta}{\partial x_\beta} \tag{5}$$

$$\frac{d\rho_i}{dt} = \sum_{j \in \Omega} m_j \left(v_\beta^i - v_\beta^j\right) \frac{\partial W_{ij}}{\partial x_\beta} \tag{6}$$

Where $\beta \epsilon \{x,y\}$, t is time and v is velocity. The momentum conservation Equation (7) is expressed in particle summation as Equation (8) using particle approximation of Equation (4).

$$\frac{dv_\alpha}{dt} = \frac{1}{\rho} \frac{\partial \sigma_{\alpha\beta}}{\partial x_\beta} \tag{7}$$

$$\frac{dv_\alpha^i}{dt} = \sum_{j \in \Omega} m_j \left(\frac{\sigma_{\alpha\beta}^i + \sigma_{\alpha\beta}^j}{\rho_i \rho_j}\right) \frac{\partial W_{ij}}{\partial x_\beta} \tag{8}$$

where $\alpha \epsilon \{x,y\}$, σ is stress and the particle approximation of strain rate is:

$$\dot{\varepsilon}_{\alpha\beta}^i = \frac{1}{2}\left(\frac{\partial v_\alpha^i}{\partial x_\beta} + \frac{\partial v_\beta^i}{\partial x_\alpha}\right) \tag{9}$$

$$\frac{\partial v_\alpha^i}{\partial x_\beta} = \sum_{j \in \Omega} \frac{m_j}{\rho_j} \left(v_\alpha^j - v_\alpha^i\right) \frac{\partial W_{ij}}{\partial x_\beta} \tag{10}$$

3. ANALYZING ORTHOGONAL CUTTING WITHOUT COOLING PROCESS

The temperature of chip-tool interface was measured [16] using thermal imaging during the orthogonal cutting process of the Ti-6Al-4V while depth of cut, rake angle, cutting speed and feed rate were 1.9 mm, 4 degrees, 750 mm/min and 0.15 mm/rev, respectively.

Table 1 shows the mechanical and physical properties of material of this cutting process. Such as elastic modulus, Poisson ratio, density, specific heat capacity, the melting point and conductivity coefficient.

TABLE 1. Work-piece and cutting tool material properties [27]

Property	Work piece	Tool
Density, ρ (kg/m^3)	4430	7800
Elastic modulus, E (GPa)	110	200
Poisson's ratio, v	.33	.3
Specific heat, C_p ($J/kg°C$)	670	-
Thermal conductivity, k ($w/m°C$)	6.6	-
T_{melt} ($°C$)	1630	-
T_{room} ($°C$)	25	25
Elastic bulk modulus, K (GPa)	107.84	-

The cutting tool was assumed a rigid body because its deformation is too small in comparison with work-piece. According to this assumption, the cutting tool and work-piece were analyzed by FE and SPH method, respectively.

The Johnson-Cook constitutive model of work-piece is:

$$\sigma=[A+B\,\varepsilon^{n}][1+C\ln\dot{\varepsilon}^{*}][1-T^{*m}] \quad (11)$$

where the parameters A, B, m, n, C are material constants and ε is the equivalent plastic strain, $\dot{\varepsilon}^{*}$ is the dimensionless parameter of the plastic strain rate and it is defined as $\dot{\varepsilon}^{*}=\dot{\varepsilon}/1\ (s^{-1})$, T^{*} is the dimensionless parameter of temperature, which is calculated from the following equation:

$$T^{*}=\frac{T-T_{room}}{T_{melt}-T_{room}} \quad (12)$$

Two set of the parameters A, B, m, n, C are given in Table 2.

Cutting parameters such as feed rate, cutting speed, depth of cut and rake angle of cutting tool are given in Table 3.

TABLE 2. Johnson-Cook constitutive model parameters of Ti-6AL-4V [30]

Set	A (MPa)	B (MPa)	n	C	m
Set 1	1098	1092	0.93	0.014	1.1
Set 2	862	331	0.34	0.012	0.8

TABLE 3. Cutting parameters and tool geometry [16]

Feed rate, f (mm/rev)	0.15
Cutting speed, V_c (mm/min)	750
Depth of cut, D (mm)	1.9
Rake angle, α (deg)	4

The FE model of cutting tool with the SPH model of work-piece is shown at Figure 1 using parameters of Table 3. The lower boundary of work-piece is fixed like the experimental test.

4. ANALYZING ORTHOGONAL CUTTING WITH COOLING PROCESS

The work-piece of Ti-6AL-4V and rigid steel cutting tool are modeled using SPH and FE method respectively at Figure 2. Cutting speed and feed rate are 300 m/min and 4 mm/rev. The time of simulation starts from entering the cutting tool to steady state of process.

The cutting process of Figure 2 was investigated with different number of particles in the volume of the work-pieces. The cutting force with different number of particles is shown at Figure 3.

Based on Figure 3, cutting force with 1.1 particles per unit volume (mm^3) is converged. The numerical value of the force with 2 particles per unit volume (mm^3) is very close to 1.1 particles but solution time was almost doubled. Therefore 1.1 particles per unit volume (mm^3) is chosen with reasonable accuracy and suitable time of solution.

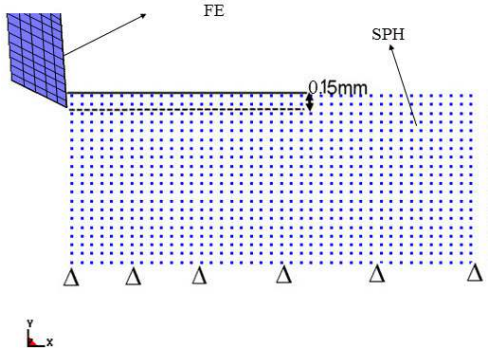

Figure 1. Modelling work-piece and cutting tool of dry orthogonal cutting process using particule and elements respectively

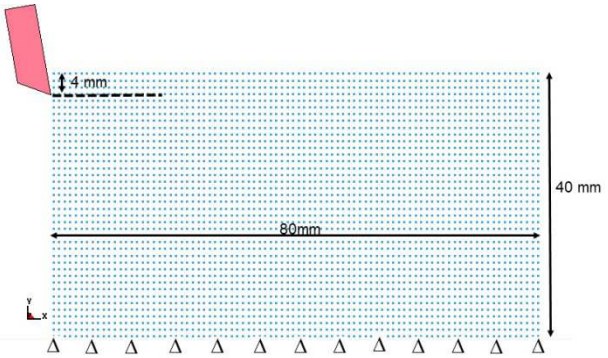

Figure 2. Tool, SPH particles, dimensions and boundary conditions of the woke-piece

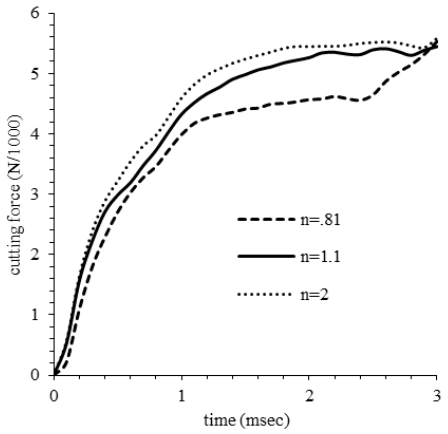

Figure 3. Converging cutting force based on the number of SPH particles of work-piece

It can be assumed that the volume of water with constant temperature is flowing on the work-piece. Adding cooling process to Figure 2 was simulated by inserting SPH particles of water at top of SPH particles of work-piece as shown at Figure 4. The feed rate of Figure 4 is same as Figure 2 and the cutting speed is 300 and 500 m/min.

5. RESULTS AND DISCUSSION

5. 1. Results of Analyzing of Non-Cooling Orthogonal Cutting Process According to Figure 5, the maximum temperature of the experimental non-cooling orthogonal cutting process [15] is approximately 200 ℃ on chip-tool interface.

According to Figure 6, The maximum temperature on chip-tool interface of the numerical model is 215 °C using set 2 of Johnson-Cook constitutive model parameters at the Table 2**.** The error of numerical temperature is 7.5% according to the experimental results.

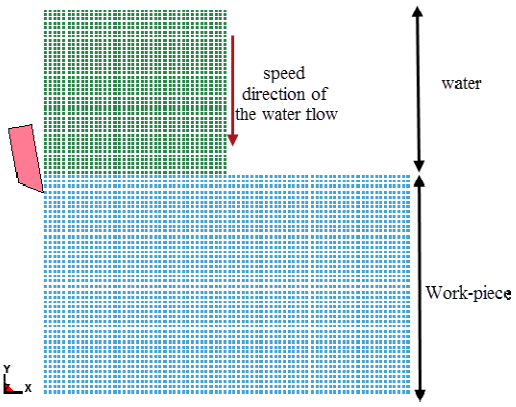

Figure 4. Cooling the orthogonal cutting process

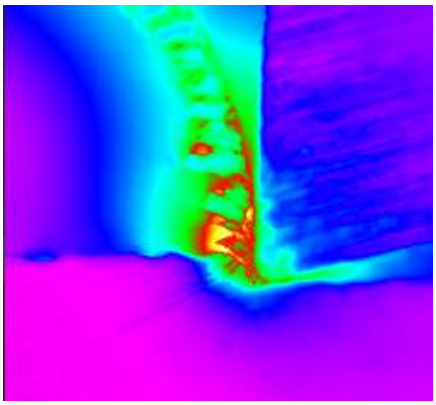

Figure 5. Colored final version of the IR image captured during the non-cooling orthogonal cutting process [16]

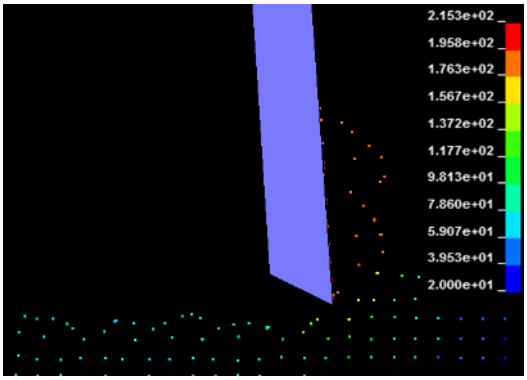

Figure 6. Temperature distribution at chip and work piece using set 2 of Johnson-Cock constitutive model parameters of Table 2.

Figure 7 shows three states of non-cooling orthogonal cutting process using set 1 of Johnson-Cook constitutive model parameters at the Table 2. The particles of the machined surface are connected with white lines.

The temperature of machined surface of Figure 7 is shown at Figure 8. According to this figure, the temperature of the machined surface initially equals to room temperature or 20°C. It increases to the maximum temperature then decreases and converges to a constant value. Based on Figures 7 and 8, the maximum temperature occurs after the formation of an indentation at the machined surface and decreases while the cutting tool moves far away from this point.

The temperature on chip-tool interface is shown at Figures 9. According to this figure, the temperature increases to the maximum value then it decreases and converges to a constant value. Peak temperature approximately repeated every 40 msec.

The maximum temperature of Figures 8 and 9 is between 305℃ to 335℃ and 385℃ to 437℃ on machined surface and chip-tool interface respectivly.

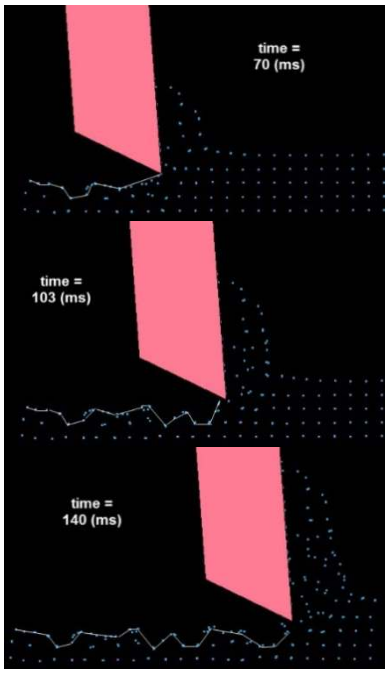

Figure 7. Configuration of machined surface of non-cooling orthogonal cutting process using set 1 of Johnson-Cook constitutive model parameters at the Table 2.

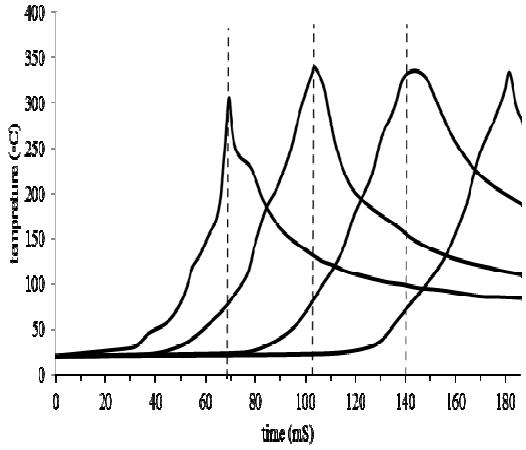

Figure 8. The temperature of the points on machined surface

The numerical temperatures are obtained while the coefficient of friction is 0.2. The temperature decreases using lower coefficient of friction.

5. 2. Results of Analyzing of Orthogonal Cutting With Cooling Process The influences of temperature and speed of water flow on the temperature of machined surface and chip-tool interface are investigated in Figures 10 to 13 while the cutting velocity is equal to 300 and 500 m/min. The speeds of water flows are 0.25, 0.5 m/s with temperature 10 and 20°C. Also temperature on machined surface and chip-tool interface of non-cooling cutting process are added to Figures 10 to 13.

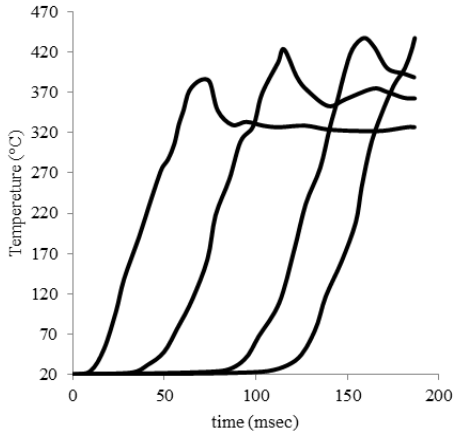

Figure 9. Temperature of particles on chip-tool interface

The word "dry" at these figures is the result of non-cooling cutting process and the letters "T" and "V" are temperature and speed of water flow respectively. The vertical axis starts from 20℃, it means that initial temperature is equal to room temperature.

Based on Figure 10, the temperature of machined surface increases with entering the cutting tool and converges to constant value in steady state of the process. The steady state temperature is 130°C without cooling process and it decreases to 104-107°C with cooling. The flow of water with low speed is more affecting on temperature of machined surface. The influence of water flow velocity is higher than its temperature.

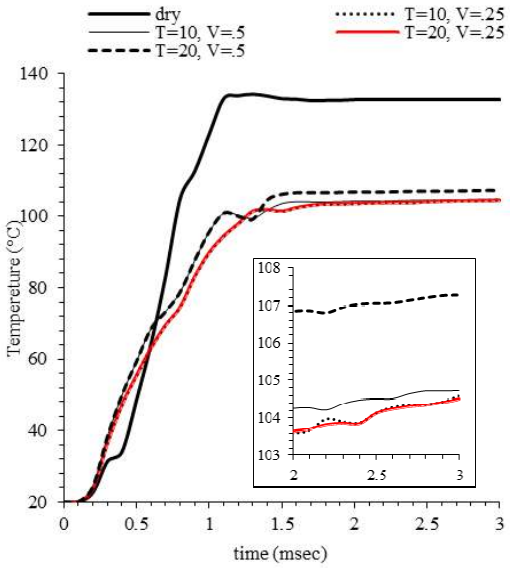

Figure 10. Effect of water flow on temperature of machined surface at cutting speed=300 m/min

The steady state temperature of non-cooling cutting process is 570°C at Figure 11 and it is 198-204°C with cooling process. Cooling process decreases the temperature of chip with ratio 0.35. The life of cutting tool increases as decreasing temperature on chip-tool interface. According to this figure, water flow at room temperature causes high decreasing in amount temperature on chip-tool interface.

According to Figures 10 and 12, the cooling process is more affective on machined surface temperature of orthogonal cutting with 300 m/min cutting velocity than 500 m/min.

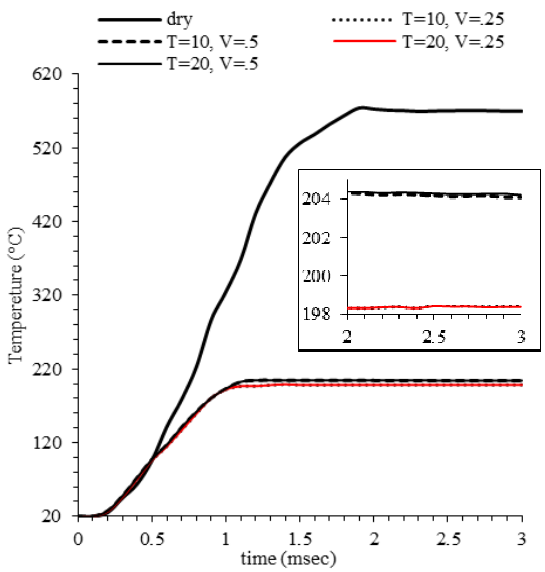

Figure 11. Effect of water flow on temperature of chip-tool interface at cutting speed = 300 m/min

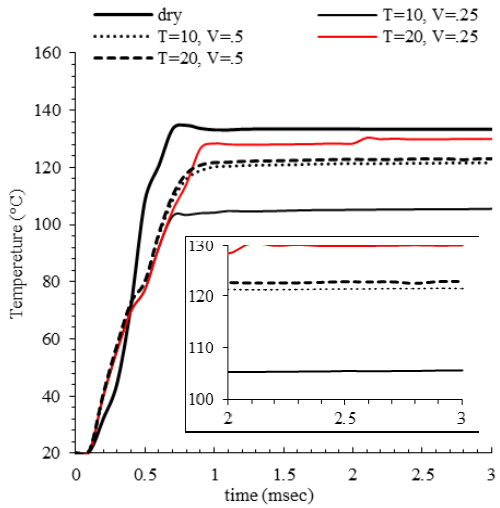

Figure 12. Effect of water flow on temperature of machined surface at cutting speed=500 m/min

According to Figures 11 and 13, flow of water with low and high velocity considerably decreases the temperature on chip-tool interface with cutting velocity 300 and 500 m/min respectively.

Cutting force of non-cooling orthogonal cutting process and cooling one with water flow are compared at Figure 14. In this figure velocity of water flow is 0.25 m/s and temperature of that is 20°C. According to this figure, cutting force decreases using cooling process.

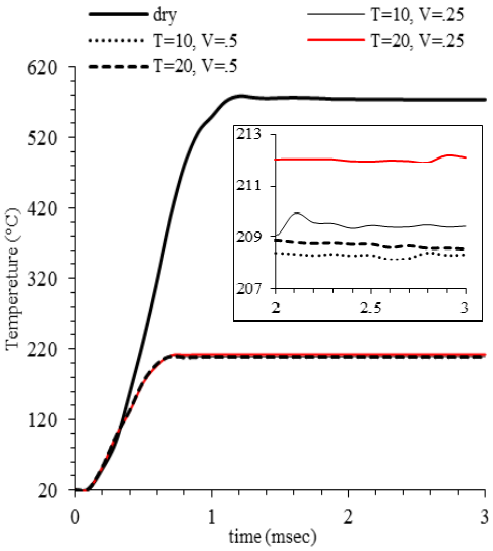

Figure 13. Effect of water flow on temperature of chip-tool interface at cutting speed = 500 m/min

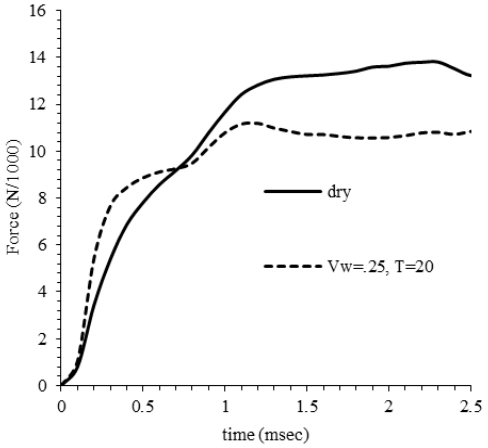

Figure 14. Cutting force of cooling and non-cooling orthogonal cutting process

6. CONCLUSION

In this paper the effect of temperature and velocity of water flow on orthogonal cutting process of Ti-6Al-4V

was investigated using SPH method. The results of the simulation using SPH method were validated by experimental results.

Temperature of orthogonal cutting process increases by entering cutting tool then converges to constant value as the process remains at steady state. The converging temperature at machined surface is lower than chip-tool interface. Temperature of machined surface and chip-tool interface at non-cooling orthogonal process are higher than process with cooling. The influence of cooling process on chip-tool interface is higher than machined surface. Cooling orthogonal cutting with water flow (low velocity and 20°C) decreases temperature and cutting force.

7. REFERENCES

1. Rajeeva D., Dinakaranb D., Kanthavelkumaran N., Austind N. "Predictions of Tool Wear in Hard Turning of AISI4140 Steel through Artificial Neural Network, Fuzzy Logic and Regression Models" ***International Journal of Engineering-Transactions A: Basic***, Vol. 31, (2018), 32-37
2. Edema F., Balogun V. A. "Energy Efficiency Analyses of Toolpaths in a Pocket Milling Process" ***International Journal of Engineering-Transactions A: Basic***, Vol. 31, (2018), 847-855
3. Balogun V. A., Edemb I. F. " Optimum Swept Angle Estimation based on the Specific Cutting Energy in MillingAISI 1045 Steel Alloy" ***International Journal of Engineering-Transactions A: Basic***, Vol. 30, (2017), 591-596
4. Patel S. S., Prajapatib J. M. " Experimental Investigation of Surface Roughness and Kerf Width During Machining of Blanking Die Material on Wire Electric Discharge Machine" ***International Journal of Engineering-Transactions A: Basic***, Vol. 31, (2018), 1760-1766
5. Safari M., Joudaki J., Emadi M., "Surface Quality in Dry Machining of 55Cr3 Steel Bars." International Journal of ISSI, Vol. 15, (2018), 33-39
6. Kline WA, Devor RE, Lindberg JR. "The Prediction Of Cutting Forces In End Milling With Application To Cornering Cuts." ***International Journal of Machine Tool Design and Research,*** Vol. 22, (1982), 7-22
7. Tsai CL. "Analysis and prediction of cutting forces in end milling by means of a geometrical model." ***International Journal of Advanced Manufacturing Technology,*** Vol. 31, (2007), 888–896
8. Li HZ, Li XP. "Milling force prediction using a dynamic shear length model." ***International Journal of Machine Tools and Manufacture,*** Vol. 42, (2002), 277–86
9. Madaj M, Píška M. "On the SPH orthogonal cutting simulation of A2024-T351 alloy." ***Procedia Cirp.***, Vol. 8, (2013), 152–157
10. Limido J, Espinosa C, Salau M, Lacome JL. SPH method applied to high speed cutting modelling. ***Internatnonal Journal Mechanical Sciences.*** Vol. 85, (2016), 2377–2388
11. Lia B., Wang Y., Li H., You H., "Modelling and Numerical Simulation of Cutting Stress in End Milling of Titanium Alloy using Carbide Coated Tool", ***International Journal of Engineering-Transactions A: Basic***, Vol. 28, (2015), 1090-1098
12. Heinstein M, Segalman D. Simulation of Orthogonal Cutting with Smooth Particle Hydrodynamics. Report, Sandia National Laboratories, USA, September 1997.
13. Stone CM, Wellman GW, Krieg RD. A vectorized elastic/plastic power law hardening material model including luders strain. Report, Sandia National Laboratories, USA, March1990.
14. Villumsen MF, *Fauerholdt TG. Simulation of Metal Cutting using Smoothed Particle Hydrodynamics*. 7th ed. LS-DYNA Anwenderforum, 2008.
15. Lu J, Chen J, Fang Q, Liu B, Liu Y, Jin T. "Finite element simulation for Ti-6Al-4V alloy deformation near the exit of orthogonal cutting." ***International Journal of Advanced Manufacturing Technology,*** Vol. 85, (2016), 2377–2388
16. Cotterell M, Ares E, Yanes J, López F, Hernandez P, Peláez G. "Temperature and strain measurement during chip formation in orthogonal cutting conditions applied to Ti-6Al-4V." ***Procedia Engineering,*** Vol. 63, (2013), 922–930
17. Kuczmaszewski J, Zagórski I, Zgórniak P. "Thermographic study of chip temperature in high-speed dry milling magnesium alloys." ***Management and Production Engineering Review,*** Vol. 7, (2016), 86–92
18. Fang F.Z., Lee L.C. LXD. "Mean Flank Temperature Measurement in High Speed Dry Cutting." ***Journal of Materials Processing Technology,*** 2005;167:119–23. Vol. 118, (2001), 301–308
19. O ' Sullivan D. CM. "Temperature measurement in single point turning", ***Journal of Materials Processing Technology***,Vol. 118, (2001), 301–308
20. Franz Obermair SP, Klammer G. "high speed minimum quantity lubrication machining of magnesium." In: Proceedings of the 6th International Conference Magnesium Alloys and Their Applications. Germany, 2005. 881–887. Wiley
21. Jeong-Du, Kim K-BL. "Surface Roughness Evaluation in Dry-Cutting of Magnesium Alloy by Air Pressure Coolant." ***Engineering***. Vol. 2, (2010), 788–792
22. Heigel JC, Whitenton E, Lane B, Donmez MA, Madhavan V. Infrared Measurement of the Temperature at the Tool-Chip Interface While Machining Ti-6Al-4V. ***Journal of Materials Processing Technology,*** Vol. 243, (2017), 123-130
23. Monaghan JJ. "Smoothed Particle Hydrodynamics." ***Annual Review of Astronomy and Astrophysics,*** Vol. 30, (1992), 543–574
24. Fadaei-Kermani E., Shojaee S., Memarzadeh R. "Numerical Simulation of Seepage Flow through Dam Foundation Using Smooth Particle Hydrodynamics Method" ***International Journal of Engineering-Transactions A: Basic*** Vol. 32, (2019), 484-488
25. Benz W, Asphaug E. "Simulations of brittle solids using smooth particle hydrodynamics." ***Computer Physics Communications,*** Vol. 87, (1995), 253–265
26. Gray JP, Monaghan JJ, Swift RP. SPH elastic dynamics. ***Computer Methods in Applied Mechanics and Engineering,*** Vol. 190, (2001), 6641–6662
27. Hiermaier S, Konke D, Stilp AJJ, Thoma K, Könke D. "Computational simulation of the hypervelocity impact of al-spheres on thin plates of different materials". ***International Journal of Impact Engineering,*** Vol. 20, (1997), 363–374
28. M.H. Farahani and N. Amanifard, S.M. Hosseini, "a high-velocity impact simulation using sphprojection method", ***International Journal of Engineering-Transactions A: Basic*** Vol. 22, (2009), 359-368
29. Hoseinpour B., Amanifard N., Basti A., " Simulation of Cold Rolling Process Using Smoothed Particle Hydrodynamics (SPH)", ***International Journal of Engineering-Transactions A: Basic*** Vol. 26, (2013), page no. 515-522
30. Zhang Y, Outeiro JC, Mabrouki T. "On the selection of Johnson-Cook constitutive model parameters for Ti-6Al-4V using three types of numerical models of orthogonal cutting" ***Procedia Cirp***. Vol. 31, (2015), 112–117

Influence of Water Cooling on Orthogonal Cutting Process of Ti-6Al-4V Using Smooth-Particle Hydrodynamics Method

M. Dehghani, A. R. Shafiei

Department of mechanical Engineering, Yazd University, Yazd, Iran

P A P E R I N F O

Paper history:
Received 15 January 2019
Received in revised form 06 June 2019
Accepted 05 July 2019

Keywords:
Orthogonal Cutting Process
Cooling
Smooth Particle Hydrodynamic

چکیده

چکیده: کنترل دمای فرآیند برش متعامد به کمک پارامترهای مختلف ازجمله سرعت برش و همچنین خنک کاری به کمک آب جهت کاهش نیروی برش، افزایش طول عمر ابزار و کاهش دمای سطح ماشین کاری شده، ضروری می‌باشد. در این مقاله، دمای سطح ماشین کاری شده و سطح براده در تماس با ابزار در فرآیند برش متعامد Ti-6Al-4V به کمک روش هیدرودینامیک ذرات هموار (SPH) بررسی شده و تاثیر خنک‌کاری با جریان آب با سرعت و دماهای مختلف بر دمای سطوح یاد شده تحلیل گردیده‌است. نتایج فرآیند برش متعامد در حالت بدون خنک‌کاری به کمک نتایج تجربی صحت سنجی شده‌است. بر اساس نتایج به دست آمده، جریان آب با سرعت ۰/۲۵ m/s و دمای ۲۰°C موجب کاهش نیروی برش، دمای سطح ماشینکاری شده و دمای سطح براده در تماس با ابزار گردیده است.

***doi**: 10.5829/ije.2019.32.08b.18*